

Version: November 26, 2018

# Exocomets in the 47 UMa System: Theoretical Simulations including Water Transport

Manfred Cuntz<sup>1</sup>, Birgit Loibnegger<sup>2</sup>, Rudolf Dvorak<sup>2</sup>

<sup>1</sup>*Department of Physics, University of Texas at Arlington,  
Arlington, TX 76019, USA*

cuntz@uta.edu

<sup>2</sup>*Institute of Astronomy, University of Vienna, Türkenschanzstr. 17  
A-1180 Vienna, Austria*

birgit.loibnegger@univie.ac.at; rudolf.dvorak@univie.ac.at

## ABSTRACT

Motivated by ongoing discoveries of features (most likely) attributable to exocomets in various systems, this study examines the dynamics of possible comets around 47 UMa. Based on the assumption that most systems hosting planets should also harbor leftovers from planet formation processes, comets are thus also expected to exist in the system of 47 UMa. This system is known to host three Jupiter-type planets; however, based on stability analyses, additional terrestrial planets in stable orbits might also be able to exist, including planets in 47 UMa's habitable zone. Furthermore, we also consider a possible 'Hilda'-planet. The aim of our study is to explore the interaction of exocomets with the Jupiter-type planets in the system and examine the probability of cometary collisions with the planets, including possible Earth-mass planets located in the habitable zone. Moreover, we investigate the transport of water onto the Earth-mass planets, including quantitative estimates. It is found that the Earth-mass planets would be able to receive some water, but much less than currently present on Earth. We also checked if the comets form families, but no families were found. Finally, the capture of comets in close orbits and the possibility of small clouds formed when comets come too close to the star and disintegrate are also part of our work.

*Subject headings:* astrobiology — circumstellar matter — comets: general — methods: numerical — protoplanetary disks — stars: individual (47 UMa)

## 1. Introduction

Following the detection of absorption lines in the spectra of  $\beta$  Pictoris (Beust et al. 1990) identified to vary on short time scales, it has been argued that these lines are produced by clouds due to the evaporation of comets passing in front of the star. Additional results for  $\beta$  Pictoris have been reported by Kiefer et al. (2014). Evidence for comets in other exoplanetary systems, also referred to as exocomets, has also been reported by, e.g., Zuckerman & Song (2012) and Welsh & Montgomery (2013). Examples include 49 Ceti, a young A-type star, as well as, e.g., HD 21620, HD 42111, HD 110411, HD 145964, and HD 183324. Generally, the evidence about possible exocomets is based on the interpretation of variable Ca II K absorption line profiles. The concept of exocomets was previously also mentioned by Ji et al. (2005), among others, from a dynamical viewpoint. Recently, Cook et al. (2016) reviewed the realistic detectability of close interstellar comets in the view of new methodologies, such as the *Large Synoptic Survey Telescope* (LSST). Note that besides exocomets, the term ‘falling evaporating bodies’ (FEBs) is sometimes used as well, especially if a more general term is preferred.

Knowledge from the Solar System indicates that comets are small icy bodies ( $\sim 0.1$  to  $\sim 100$  km in diameter) that represent leftovers from planet formation (Brasser 2008; A’Hearn 2011). In fact, they may have played a pivotal role in the delivery of water and basic organic substances from the outskirts of the Solar System to the terrestrial planets, especially Earth and perhaps Mars as well; see, e.g., Raymond & Izidoro (2017) for recent theoretical results. Nevertheless, the efficiency of water transport by planetesimals, asteroids, and comets is still part of previous and ongoing discussions (e.g., Genda & Ikoma 2008; Raymond & Izidoro 2017). The latter authors argue that the availability of comets to the inner stellar systems is a natural consequence of the formation of giant planet(s); if correct, this result would be highly relevant beyond the inherent physics and biochemistry of the Solar System.

In the Solar System, cometary bodies have three known reservoirs, which are: the Oort cloud, the Kuiper belt, and the Main belt (e.g., Hsieh & Jewitt 2006), which originated from gravitational interactions of the planetesimals and asteroids with the giant planets during the phase of planet formation (Brasser 2008). Assuming that gravitational scattering is common during the stage of planet formation we conclude, that there have to be reservoirs for small bodies in other planetary systems, too. As mentioned above, features attributable to exocomets have been observed in the spectra of many stars, with focus on A-type stars (e.g., Zuckerman & Song 2012; Welsh & Montgomery 2013). Those systems are around mainly young stars ( $\sim 5$  Myr), which are supposedly also accompanied by planet formation. However, as pointed out by (e.g., Cook et al. 2016, and references therein) comets are expected in other systems as well, including interstellar space. Very recently, Rappaport et al. (2018)

reported the first observations of (likely) transiting exocomets detected by *Kepler*, hosted by KIC 3542116 and KIC 11084727, both of spectral type F2 V.

The aim of the present work is to examine the dynamics of comets in the extrasolar system of 47 UMa. This system has some notable similarities to the Solar System, including the spectral type and mass of the central star and the dominance of two giant planets, which decisively impact the system’s innermost parts. Generally, we want to study if the transport of water and prebiotic material could be possible toward Earth-type planets, including planets located in 47 UMa’s habitable zone (HZ). In particular, material losses by comets will be calculated as well in order to make predictions about the observability of comets in this type of system. The structure of the 47 UMa system, including the previous discovery of planets as well as the extent of the stellar HZ, will be discussed in Sect. 2. The adopted methods and the numerical setup are explained in Sect. 3. Our results and discussion are given in Sect. 4. Section 5 conveys our summary and conclusions.

## 2. The 47 UMa System

The system of 47 UMa has been regarded as showing significant similarities to the Solar System<sup>1</sup>. This assessment readily applies to the stellar spectral type, effective temperature, metallicity, and mass; see Table 1. In this study, we will use  $T_{\text{eff}} = 5890$  K,  $M = 1.03 M_{\odot}$ , and  $R_{*} = 1.17 R_{\odot}$ ; these values have previously been determined by Henry et al. (1997) and Gonzalez (1998), with updates by Kovtyukh et al. (2003) and van Belle & von Braun (2009).

Previous studies have shown that 47 UMa harbors (at least) three Jupiter-type planets in low-eccentricity orbits, designated as 47 UMa b, 47 UMa c, and 47 UMa d, with semi-major axes of 2.1 au, 3.6 au, and 11.6 au (see Table 2). Those detections have been made by Butler & Marcy (1996), Fischer et al. (2002), and Gregory & Fischer (2010), respectively, prominently based on the radial velocity method; 47 UMa d was identified using a Bayesian periodogram applied to the data. Especially 47 UMa b and 47 UMa c are found to be in almost circular orbits; the planetary eccentricities are given as 0.032 and 0.098, respectively. Thus, 47 UMa b and 47 UMa c are often regarded as Jupiter and Saturn analogs, albeit that they are more massive and at closer proximity to their host star, compared to Jupiter and Saturn to the Sun. Scenarios for the formation of the giant planets around 47 UMa have

---

<sup>1</sup>This statement was particularly genuine prior to the discovery of the third Jupiter-type planet, 47 UMa d. However, 47 UMa d is located at a relatively large distance from the star, and thus is not expected to significantly impact the inner part of the 47 UMa system, including its HZ.

previously been described by Thébault et al. (2002) and Kornet et al. (2002).

Estimates of 47 UMa’s age are available as well. Stellar ages can, for instance, be obtained through analyzing the age-activity relations or isochrone fitting (Henry et al. 1997). In case of 47 UMa, the age-activity relationship of Donahue (1993) implies 7 Gyr, in agreement with the estimate of 6.9 Gyr by Edvardsson et al. (1993) from isochrone fitting and work by Ng & Bertelli (1998). More recent work by Saffe et al. (2005) based on a variety of methods, including those previously used by other authors, however, indicates  $\sim 6.03$  Gyr. Therefore, we will adopt 6 Gyr in this study. Thus, 47 UMa is considered a main-sequence star, although it already underwent a noticeable evolutionary process, steadily approaching the subgiant stage.

Another important aspect pertains to the calculation of 47 UMa’s HZ<sup>2</sup>. Kopparapu et al. (2013) provided detailed calculations for the limits of stellar HZs using different criteria. Based on this work, the inner and outer limits for 47 UMa’s general HZ (i.e., conservative estimates) are given as 1.19 au and 2.04 au, respectively, whereas the limits for 47 UMa’s optimistic HZ are identified as 0.91 au and 2.13 au, respectively. The latter values correspond to the climatological settings of recent Venus / early Mars (RVEM) in the Solar System. However, in case of 47 UMa, the outer part of the HZ is unavailable for hosting planets owing to the influence of 47 UMa b, the innermost system planet, due to the initiation of orbital instabilities. The truncation occurs at about  $\lesssim 1.6$  au, a number somewhat depending on the values adopted as system parameters. Detailed simulations on the truncation of 47 UMa’s HZ have been given by, e.g., Noble et al. (2002), Goździewski (2002), and Laughlin et al. (2002). Previous theoretical studies about hypothetical Earth-mass planets in the 47 UMa system, including analyses of orbital stability, have been obtained by Jones et al. (2001), Cuntz et al. (2003), Franck et al. (2003), Asghari et al. (2004), and Ji et al. (2005).

---

<sup>2</sup>Previously, 47 UMa was studied by Turnbull & Tarter (2003) for its potential regarding the *Search for Extraterrestrial Intelligence* (SETI), and it received an overall positive assessment. However, they still decided not to include it in their *Catalog of Habitable Stellar Systems* (HabCat), in part because 47 UMa’s outer part of its HZ is unavailable for hosting planets. Nevertheless, 47 UMa continues to be of great interest to the astrobiology research community.

### 3. Methods and Numerical Setup

#### 3.1. Comets

As part of our study we assume that 47 UMa harbors an Oort-type cloud of comets at the system’s outskirts. These comets are expected to be gravitationally disturbed by, e.g., a passing star or through galactic tidal forces, which will result in highly eccentric cometary trajectories allowing the comets to enter the system’s inner domain. Cometary orbits and mechanisms of injections of comets have previously been studied based by numerous authors (e.g., Fouchard et al. 2007, 2017; Rickman et al. 2008; Feng & Bailer-Jones 2015, among others). The main goal of this study is to investigate how comets in the 47 UMa system would be scattered or eventually captured by the system’s planets. In particular, we are interested in exploring the probability of cometary collisions. Specifically, we focus on cometary collisions with a fictitious planet assumed to orbit within 47 UMa’s HZ. Therefore, we record the impact angles and velocities of the comets’ collisions, which will be used for further analyses, including estimates of upper limits for the amount of water transported to the planets.

In our integrations we include the three known planets of 47 UMa (see Table 2) as well as an additional (hypothetical) fourth planet assuming three cases of initial semi-major axes:

$$a_1 = 1 \text{ au}$$

$$a_2 = 1.25 \text{ au}$$

$$a_3 = 1.584 \text{ au} \quad (\text{‘Hilda’-like orbit})$$

We consider tens of thousands of fictitious comets assumed as massless<sup>3</sup>. These comets have been evenly distributed in a sphere with initial conditions given in Table 5. Furthermore, an isotropic angular distribution has been assumed for the cometary initial conditions owing to the lack of detailed information about exocomets in that system. As the comets have been assumed to originate from an Oort Cloud analog, they have been placed in nearly hyperbolic orbits; the integration time was set to 1 Myr. Whenever a comet was ejected from the system or underwent a collision, another comet was inserted with the same ‘initial’ conditions as the previous comet. Since at the time of insertion the configuration of the planets has changed, the newly inserted comet will exhibit a different dynamics.

---

<sup>3</sup> Comets assumed as massless indicates that the star and the system planets (known or hypothetical) are able to exert gravitational forces toward the comets but not vice-versa. Furthermore, the comets do not gravitationally interact with one another.

We also track the comets’ semi-major axes and eccentricities to determine if a comet was captured into a long or short periodic orbit. Moreover, we will inspect our results for analogs of cometary families as known for our Solar System. The integration of the equations of motion was performed using Lie-transformation with adaptive step size control, which is particularly accurate when modeling close encounters and collisions of celestial bodies (e.g., Hanslmeier & Dvorak 1984; Eggl & Dvorak 2010). The integrations were performed with a highly variable step size. The step size for the innermost planet is at the beginning 10 days for a step-to-step precision of  $10^{-13}$ . However, due to the automatic step size control as part of the Lie-integrator, it changes according to the involved masses and their mutual distances. This means that at close encounters, i.e., just prior to a collision, the step size attains values as small as a few hours.

### 3.2. A ‘Hilda’-planet

In the asteroid belt between Mars and Jupiter there exists an interesting accumulation of asteroids residing in the region between 3.7 au and 4.2 au. They orbit in a zone of mean-motion resonance (MMR) with Jupiter the one in the orbital resonance 3:2. The term *Hilda asteroids* — nowadays more than 1000 are known — was coined after asteroid 153, Hilda, was discovered by Johann Palisa<sup>4</sup> in 1875. Previous theoretical explorations of ‘Hilda’ analogs in the 47 UMa system have been given by Laughlin et al. (2002) and Ji et al. (2005).

Because of the existence of 47 UMa b, the innermost gas giant in the system of 47 UMa with properties akin to Jupiter (albeit having a notably smaller semi-major axis, i.e., 2.1 au versus 5.2 au; see Table 2), we also explore the orbital properties of a hypothetical terrestrial planet assumed in the region of the 3:2 MMR. This planet would still be located in 47 UMa’s HZ, see Kopparapu et al. (2013), even though its outer segment (i.e., beyond  $\simeq 1.6$  au) is unavailable due to the disturbances given by 47 UMa b (e.g., Noble et al. 2002; Goździewski 2002). In the following, we investigate the interaction of the comets with this planet as well, including the possible proliferation of water.

---

<sup>4</sup>see <https://ssd.jpl.nasa.gov/sbdb.cgi?sstr=Hilda> for details.

## 4. Results

### 4.1. Collisions

The aim of our study is to investigate the dynamics of (hypothetical) comets in the system of 47 UMa, known to harbor three Jupiter-type planets with two of them located closer to the host (i.e., at 2.1 au and 3.6 au, respectively) compared to Jupiter to the Sun. Additionally, we consider some fictitious Earth-mass planets; see Sect. 3.1. Hence, we will evaluate the statistics of collisions of comets with the planets (known or fictitious) around 47 UMa. Moreover, we will investigate the stability of the 3:2 resonance with the most massive planet in the system (47 UMa b) that is in analogy to the dynamics of the Hilda asteroids in the Solar System (see Section 4.6).

A collision between a massless body (comet) and the Earth-mass planet is considered an incident where the massless body comes as close to the terrestrial planet as  $r_{\text{Earth}}$ , taken as 6370 km. At this distance, the comet would hit the surface of the Earth-like planet. Clearly, the extent of the comet core itself can be assumed as negligible.

A key motivation for our study of cometary collisions is that we want to explore the possible water transport by comets to the Earth-mass planets. In Figure 1 we show the number of collisions of comets with the four planets included in our integrations. Clearly, the probability of a collision strongly depends on the initial conditions of the comets (i.e., initial inclination and initial eccentricity). Comets with relatively low initial eccentricities are unable to reach the inner planetary system. Consequently, they cannot collide with any of the Earth-mass planets put close to or within the HZ unless they are scattered inward by the 47 UMa system planets. In fact, the most massive planet in the system, 47 UMa b, experiences the most collisions. Furthermore, it is more likely for comets of low initial inclinations to collide with any of the planets. This behavior is found for all initial configurations; it is also visible in Figure 2. It occurs as a result from the choice of initial parameters for the planets orbiting 47 UMa, which in lack of knowledge about their inclinations have been placed in coplanar orbits.

In Figure 3, we depict cometary collisions with the Earth-mass planet at different locations. The surface of the planet is marked with a green line. One can see that comets cross this line, indicating that collisions have occurred. During these collisions transport of water and organic material is expected to take place. Interestingly, the closer the Earth-mass planet is moved toward the most massive planet (47 UMa b), the lesser number of cometary collisions occur. The Earth-mass planet is placed first at 1 au, and at this orbit it suffers from most collisions. Putting it in an orbit closer to 47 UMa b considerably reduces the number of collisions (see Figure 3).

When we put the Earth-mass planet at 1.584 au (an orbit in 3:2 MMR resonance with 47 UMa b analog to the Hilda family of asteroids in the Solar System), no collisions are found to occur at all, which makes water transport to a Hilda analog through cometary collisions in 47 UMa impossible. We conclude that the proximity to the most massive planet in the system and the occurrence of orbital resonances prevent Earth-mass planets in the distance range-as-evaluated from being hit by comets; all comets are scattered away by 47 UMa b. This behavior indicates that (1) Earth-mass planets in the 47 UMa system in resonance with the most massive planet can be orbitally stable, and (2) those planets will be spared from collisions with comets or other objects entering the system on high eccentric trajectories owing to the gravitational influence and scattering caused by 47 UMa b. Thus, the biggest planetary object, partly due to the virtue of resonances, acts like a shield, protecting the inner planetary system.

#### 4.2. Water transport

In order to estimate an upper limit for water transport by comets, we assume that a comet consists by 20% of water (Fulle et al. 2017). For simplicity, we also assume that all the water transported by the comet is transferred to the fictitious terrestrial planet in case of a collision. This is only a first step in the framework of our envisioned studies, and we are aware that the collision geometry will probably reduce the amount of transferred water by a significant extent. The collision details such as impact angles and impact velocities are stored from our calculations; in fact, more detailed collision studies are anticipated.

We made the following assumptions for the terrestrial planet orbiting at 1 au: A comet has an estimated mass of  $10^{14}$  kg, which is approximately the the average mass of comets measured in the Solar System. In the beginning we put 100 comets on eccentric trajectories about the star. They amount to a total mass of  $10^{16}$  kg, which entails an estimated water content for the total cometary population of  $2 \times 10^{15}$  kg. If a comet is engulfed by the star or is ejected from the system, it is replaced by a new comet. This can add up to a very high number of comets intruding the planetary system during our integrations. Earth’s oceans consist of  $1.5 \times 10^{21}$  kg of water. This means that in our initial comet population, 0.00013% of Earth’s oceans are incorporated. This amount of water, for example, would also correspond to 8.8% of the combined body of water<sup>5</sup> of the Great Lakes, located on the Canada – United States border.

---

<sup>5</sup>The total amount of water for the Great Lakes has been estimated as 5439 cubic miles. Information as reported by the U. S. Environmental Protection Agency; see <http://www.epa.gov/glnpo/physfacts.html>

For example, we calculated the transported mass of water for comets with initial semi-major axis of 80 au and no inclination: 118,557 comets have been induced in addition to the initially 100 comets of the system. This amounts to a total number of 118,657 comets integrated for 1 Myr in total, with an estimated total mass of  $1.2 \times 10^{19}$  kg and a total water content of  $2.4 \times 10^{18}$  kg (expressed in Earth’s oceans: 0.16%). Of these 118,557 comets, 9 collided with the Earth-mass planet depositing  $1.8 \times 10^{14}$  kg of water, which corresponds to 0.000012% of Earth’s oceans or 0.8% of the Great Lakes. This amount of water is delivered during an integration time of 1 Myr.

If this value is extrapolated to the age of 47 UMa, given as 6 Gyr (see Table 1), a total amount of water of  $1.1 \times 10^{18}$  kg (i.e., 0.073% of Earth’s oceans or 48.5 times the water of the Great Lakes) is derived, thus able to reach the surface of the terrestrial planet at 1 au. For the total number of comets considered with initial semi-major axes of 80 au, the following values are obtained: 2,174,536 comets plus 1900 initial ones amount to 2,176,436 comets. In this combined number of comets, a total mass of water given as  $4.4 \times 10^{19}$  kg is included. For this configuration we observed 12 collisions. If perfect merging is assumed, and the delivery of the total amount of water from the comets to the Earth-mass planet (orbiting at 1 au in this scenario) occurs as said,  $2.4 \times 10^{14}$  kg of water are delivered to the planet. This corresponds to 0.000016% of Earth’s oceans or 1.1% of the water of the Great Lakes, transferred to the planet during 1 Myr. Extrapolating this value to an age of 6 Gyr results in  $1.4 \times 10^{18}$  kg of water, equivalent to 0.093% of Earth’s oceans or 61.7 times of the water contained in the Great Lakes.

Taking all the comets with initial semi-major axes between  $80 \text{ au} < a_{\text{ini,comet}} < 200 \text{ au}$  into account, only 12 collisions with the Earth-mass planet are observed at 1 au. Comets with higher initial semi-major axes are found not to be able to reach the inner planetary system and collide with the terrestrial planet. These calculations have been repeated for the Earth-mass planet at 1.25 au and the ‘Hilda’-planet. The outcomes are given in Table 2. We found that the ‘Hilda’-planet does not receive any water because it does not encounter any collisions with the comets. This convincingly demonstrates the shielding effect of the most massive planet, 47 UMa b. Additionally, the 3:2 resonance — where the ‘Hilda’-planet resides — protects that planet from collisions with the cometary bodies.

Since perfect merging has been assumed, i.e., the transfer of the total amount of water of a comet to the Earth-mass planet, only an upper limit of water reaching the surface of the Earth-type planet inserted in the system of 47 UMa is described. For the 47 UMa system, we realize that the number of collisions with the small planet orbiting inside the three known system planets is very small. Especially the most massive planet, 47 UMa b, orbiting at 2.1 au from the star, scatters most of the comets away, thus preventing them from entering the outer

HZ at about 1.6 au, the approximate distance of the ‘Hilda’-planet. Water transport has previously been estimated by Bancelin et al. (2015, 2017), who considered water transport via asteroids to planets in binary star systems.

### 4.3. Captured comets

Motivated by the findings of two distinct families of comets in the  $\beta$  Pictoris system (see Kiefer et al. 2014), we also tried to distinguish between different cometary families in the 47 UMa system among the comets scattered into orbits of low semi-major axes and eccentricities; these comets were considered captured. Unfortunately, it was not possible to determine different families of comets in this system. Nevertheless, the capture of comets into orbits was noted in our simulations due to gravitational scattering by the massive planets of the system, especially 47 UMa b.

Our integrations showed that the capture of comets into orbits with a low semi-major axis and eccentricity is possible. This can result in comets of short-periodic orbits, maybe forming some kinds of family analogs to our Solar System. The lower the eccentricity of the intruding comet, the higher is the probability to be scattered to a less eccentric orbit (see Figure 4). Comets with initially higher eccentricities are able to penetrate deeper into the planetary system and reach the orbit of the most massive planet 47 UMa b at a distance of 2.1 au. Due to its mass this planet has the biggest influence on orbits of comets entering the inner part of the 47 UMa system.

If we also add the Earth-mass planet to the system, the big picture doesn’t change. The reason is that this hypothetical planet, located closer than 47 UMa b to the star, has barely any influence on the cometary scattering process. Interestingly, the number of captured comets decreases for the Earth-mass planet placed at 1.25 as well as 1.584 au, relative to the case for the Earth-mass planet at 1.0 au.

### 4.4. Encounters with the planets

Encounters of the comets with the planets are important for facilitating scattering processes. A close encounter is defined as the flyby of a comet within 5 Hill radii of the planet. A close encounter leads to a change of the comet’s trajectory and thus may lead to a capture or collision with one of the planets, or the comet’s ejection from the system. When assumed that comets in the proximity of the star start to lose mass by degassing, it can thus also be assumed that material may be transferred from the comet to the planet in case of a close

encounter.

The latter will lead to the transfer of cometary material onto the planet, including, e.g., meteorite showers. In Figure 5 we show the number of close encounters with the 4 planets in the 47 UMa system (i.e., the 3 known planets and a hypothetical ‘Earth’). The most massive planet, 47 UMa b, experiences the most close encounters. This result depends on the initial conditions of the comets, as expected. Comets with an initially low eccentricity will not come as close to the star, largely because of the presence of 47 UMa b. Thus, the number of encounters is remarkably smaller than for comets with an initially high eccentricity. As already mentioned, due to the system’s structure, the interaction between the planets and comets with initially high inclinations is sparse, which is the reason for the relatively low number of close encounters between those objects.

#### 4.5. Orbital distribution of comets

The distribution of orbital elements of the trajectories (i.e., semi-major axis versus eccentricity) identified for the comets after an integration time of 1 Myr is shown in Figure 6. The integrated system included an Earth-mass planet originally placed at 1 au. Furthermore, the comets started with an initial semi-major axis of 80 au. Regarding the initial distribution, half of the comets were started in retrograde orbits relative to the 47 UMa planetary system. It is noteworthy that at the end of the integration time, half of the comet population remained in retrograde orbits despite the shorter interaction time with the planets due to their trajectories.

Our simulations did not reveal different families of comets in the system of 47 UMa; however, we are inclined to conclude that the system might contain different comet populations. There is a small population of comets being scattered to orbits with very low eccentricities and small semi-major axes, which might be analogous to the Jupiter-family comets of the Solar System (see Figure 6, left panel). An even bigger population is found with eccentricities between 0.3 and 0.6, but still small semi-major axes with values  $< 40$  au (Figure 6, middle panel). This intermediate population of comets appears to be a bridge of the Jupiter-family-type comets to the Halley-type comets revealed by the results of our calculations. The latter yields the biggest number of comets identified. They have relatively high eccentricities ( $e > 0.6$ ) and their semi-major axes are mostly larger than 50 au (Figure 6, right panel).

#### 4.6. The ‘Hilda’-Planet

We also explored the influence of a planet in a Hilda-like orbit (see ref 3.2), originally placed at 1.584 au. In order to identify the stability regions for that additional planet, we checked the entire region of the 3:2 MMR assuming a cloud of fictitious comets as before. In terms of their initial conditions, have been equally distributed from  $1^\circ$  to  $360^\circ$  in the difference of the perihelion asteroids – gas giant, i.e.,  $\Delta(\omega_{\text{giant}} - \omega_{\text{planet}})$ . In varying the semi-major axes, the eccentricities, and the inclinations of the comets, we were able to identify the regions of greatest stability.

Figure 7 depicts one of the diagrams semi-major axes versus the differences in the perihelion longitude between the gas giant and the fictitious comets. From orbital consideration of the 3:2 MMR, we expect two windows: the first around  $85^\circ$  and the second around  $215^\circ$ . In fact, we can see from the plot that in our numerical integrations two main stable windows appear about those values. Between the windows, some stable orbits for ‘Hilda’-planets can be seen; however, these objects are expected to escape after longer times of integration. A zoom of the two windows of Figure 7 is depicted in Figure 8.

Finally, we started a fictitious ‘Hilda’-planet in the second stable window, which is again within the system’s HZ (see Table 1). The integration time was set to 10 Myr and the orbital elements of all planets were checked regarding stability with special emphasis on the ‘Hilda’-planet and the nearby gas giant, 47 UMa b. Figure 9 depicts the orbital evolution for the ‘Hilda’-planet during the first Myr (left upper plot). There is a main period visible, which is  $P \sim 70$  kyr with two different amplitudes for the semi-major axis. After 9 Myr a slight change in the periods occurs; for the gas giant the signal is akin to a diminishing period with time (right plots).

In Figure 10 we plotted the difference  $\tilde{\omega}_{\text{planet}} - \tilde{\omega}_{\text{Hilda}}$ ; it indicates how the orbit of the fictitious ‘Hilda’-planet is connected to one of the system planets, i.e., 47 UMa c. The stability of the ‘Hilda’-planet is caused by the coupling of this planet at 1.58 au to the Jupiter-type planet at 2.1 au. The reason for the stability is due to the secular apsidal resonance (1:1, with a period of 20 kyr) also observed for other planetary systems as described in earlier work (e.g., Goździewski 2003; Ji et al. 2003).

### 5. Summary and Conclusions

The focus of this study is to explore the orbital dynamics of possible exocomets in the system of 47 UMa. This star exhibits various similarities to the Sun, as evidenced by its spectral type, effective temperature, metallicity, and mass — although it has been determined

that 47 UMa is more evolved compared to the Sun while still being on the main-sequence; see Sect. 2 for references and details. Furthermore, 47 UMa is host of three Jupiter-mass planets, discovered between 1996 and 2010. In addition, simulations have indicated the possibility of Earth-mass planets in the system (e.g., Thébault et al. 2002), although there are no discoveries yet. These putative terrestrial planets are at semi-major axes  $a \lesssim 1.5$  au, with the range of those results somewhat depending on the adopted model parameters. In our work, we consider hypothetical terrestrial planets with initial distances of 1 au, 1.25 au, and 1.584 au; the later object is also referred to as ‘Hilda’-planet. Our work is motivated by previous acclaimed detections of comets in various extrasolar systems, as reported by, e.g., Kiefer et al. (2014), Cook et al. (2016), Rappaport et al. (2018), among others.

Our sets of integrations yielded the following results:

- (1) The general behavior of cometary collisions regarding the hypothetical terrestrial planets is determined by 47 UMa b, the closest in and most massive of three Jupiter-type 47 UMa planets. This planet is significantly closer to 47 UMa’s HZ (compared to Jupiter in the Solar System), and thus a larger impact on the orbital stability of HZ Earth-mass planets.
- (2) As expected, the probability of a comet-planet collision was found to depend on the cometary initial conditions (i.e., inclination and eccentricity). Comets with relatively low initial eccentricities were unable to reach the inner planetary system; thus, there were unable to collide with any of the assumed Earth-mass planets unless they were scattered inward by the 47 UMa system planets.
- (3) Regarding the Earth-mass planet at 1.584 au (i.e., the ‘Hilda’-planet), no collisions are found to occur at all, which makes water transport to Hilda analogs through cometary collisions in a system akin to 47 UMa impossible.
- (4) Motivated by the structure of the Solar System, we also checked if the comets form families; however, no families were found. But the system might contain different comet populations. According to our simulations, there is a small population of comets being scattered to orbits with very low eccentricities and small semi-major axes, which might be analogous to the Jupiter-family comets.
- (5) Moreover, it was found that comets can be captured in close orbits, implying that they may disintegrate as part of their future dynamic evolution.

Thus, the overall picture implies that — following the premise that all the water on the planets arises from cometary impacts — Earth-mass planets in the 47 UMa system are expected to constitute “land worlds”. Those planets would still be potentially habitable. Land worlds, though from a global perspective considered unlikely, as argued by Simpson

(2017), are expected to possess a range of well-pronounced atmospheric and geodynamic features. For example, Abe et al. (2011) studied those planets (also referred to as “desert worlds”) via three-dimensional global climate models and concluded that they imply wider HZs compared to Earth-sized planets for a given star. Based on this work, Venus — at a distance of 0.723 au (semi-major axis), which would translate to 0.88 au for the 47 UMa system — might have been habitable as recently as 1 billion years ago.

In a separate approach, Vermeij (2017) pointed out that studies about the history of terrestrial biological evolution showed that significant evolutionary innovation occurred as a consequence of land colonization, which is Earth-based evidence for the significance of land words in biological contexts. As indicated in this work, 11 of 13 major post-Ordovician innovations appeared first or only on land. Although the evolutionary patterns of life on exoplanets (if present) are expected to be fundamentally different from terrestrial life forms, land worlds still deserve further attention.

On the other hand, terrestrial planets located in 47 UMa’s HZ might still be able to harbor considerable amounts of water (i.e., on the surface or subsurface), despite the relative inefficiency of exocomets if other processes for the origin of water would have occurred. For example, Raymond & Izidoro (2017) in their study about the Solar System argued that water in the inner part of the system could have been delivered as a by-product of the giants’ formation process. They found that as a gas giant’s mass increases, the orbits of nearby planetesimals (supposedly, many of them with considerable water contents) are destabilized and gravitationally scattered in all directions, including the domain of terrestrial planets in the center star’s vicinity.

Therefore, regarding 47 UMa, even if the amount of water proliferated to Earth-mass planets via exocomets is small (or zero, or close to zero, as for the ‘Hilda’-planet), there are still prospects for water-based habitability. In fact, some previous studies for the Solar System comets of, e.g., Halley, Hyakutake, Hale-Bopp, and 67P/Churyumov-Gerasimenko indicate that Earth’s water originating solely from comets as implausible, considering their isotope ratios of deuterium to protium (D/H ratio) measurements; see Eberhardt et al. (1995), Bockelée-Morvan et al. (1998), Meier & Owen (1999), and Altwegg et al. (2015), respectively. A recent review by Alexander et al. (2018) conveys D/H values for a total of 13 Solar System comets, encompassing both Oort Cloud and Jupiter Family comets. Typically, the D/H ratios were found to be a factor of 1.5 to 3 times higher than the terrestrial value, which is  $1.49 \pm 0.03 \times 10^{-4}$  (Lécuyer et al. 1998). However, exceptions exist. For example, the D/H ratio of C/2014 Q2 (Lovejoy) perfectly agrees with that of Earth (Biver et al. 2016).

Thus, it is both timely and appropriate to continue developing different scenarios for the proliferation of water to possible terrestrial planets in systems such as 47 UMa, which

are characterized by the existence of giant planets as well as the possibility of terrestrial planets in the systems' HZs.

This research is supported by the Austrian Science Fund (FWF) through grant S11603-N16 (B. L. and R. D.). Moreover, M. C. acknowledges support by the University of Texas at Arlington. Additionally, we wish to thank the anonymous referee for their helpful comments.

## REFERENCES

- Abe, Y., Abe-Ouchi, A., Sleep, N. H., & Zahnle, K. J. 2011, *Astrobiol.* 11, 443
- A’Hearn, M. F. 2011, *ARA&A*, 49, 281
- Alexander, C. M. O’D., McKeegan, K. D., & Altwegg, K. 2018, *Space Sci. Rev.*, 214, 36
- Altwegg, K., Balsiger, H., Bar-Nun, A., et al. 2015, *Science*, 347, 387
- Asghari, N., Broeg, C., Carone, L., et al. 2004, *A&A*, 426, 353
- Bancelin, D., Pilat-Lohinger, E., Eggl, S., et al. 2015, *A&A*, 581, A46
- Bancelin, D., Pilat-Lohinger, E., Maindl, T. I., Ragossnig, F., & Schäfer, C. 2017, *AJ*, 153, 269
- Beust, H., Vidal-Madjar, A., Ferlet, R., & Lagrange-Henri, A. M. 1990, *A&A*, 236, 202
- Biver, N., Moreno, R., Bockelée-Morvan, D., et al. 2016, *A&A*, 589, A78
- Bockelée-Morvan, D., Gautier, D., Lis, D. C., et al. 1998, *Icarus*, 133, 147
- Brasser, R. 2008, *A&A*, 492, 251
- Butler, R. P., & Marcy, G. W. 1996, *ApJ*, 464, L153
- Cook, N. V., Ragozzine, D., Granvik, M., & Stephens, D. C. 2016, *ApJ*, 825, 51
- Cuntz, M., von Bloh, W., Bounama, C., & Franck, S. 2003, *Icarus*, 162, 214
- Donahue, R. A. 1993, Ph.D. thesis, New Mexico State University
- Eberhardt, P., Reber, M., Krankowsky, D., & Hodges, R. R. 1995, *A&A*, 302, 301
- Edvardsson, B., Andersen, J., Gustafsson, B., Lambert, D. L., Nissen, P. E., & Tomkin, J. 1993, *A&A*, 275, 101
- Eggl, S., & Dvorak, R. 2010, in *Dynamics of Small Solar System Bodies and Exoplanets*, eds. J. Souchay & R. Dvorak, *Lecture Notes in Physics*, Vol. 790 (Berlin: Springer), p. 431
- Feng, F., & Bailer-Jones, C. A. L. 2015, *MNRAS*, 454, 3267
- Fischer, D. A., Marcy, G. W., Butler, R. P., Laughlin, G., & Vogt, S. S. 2002, *ApJ*, 564, 1028

- Fouchard, M., Froeschlé, C., Breiter, S., Ratajczak, R., Valsecchi, G. B., & Rickman, H. 2007, *Lecture Notes in Physics*, eds. D. Benest et al., Vol. 729 (Berlin: Springer), p. 273
- Fouchard, M., Rickman, H., Froeschlé, Ch., & Valsecchi, G. B. 2017, *Icarus*, 292, 218
- Franck, S., Cuntz, M., von Bloh, W., & Bounama, C. 2003, *IJAsB*, 2, 35
- Fulle, M., Della Corte, V., Rotundi, A., et al. 2017, *MNRAS*, 469, S45
- Genda, H., & Ikoma, M. 2008, *Icarus*, 194, 42
- Gonzalez, G. 1998, *A&A*, 334, 221
- Goździewski, K. 2002, *A&A*, 393, 997
- Goździewski, K. 2003, *A&A*, 398, 315
- Gregory, P. C., & Fischer, D. A. 2010, *MNRAS*, 403, 731
- Guillot, T. 1999, *Science*, 286, 72
- Hanslmeier, A., & Dvorak, R. 1984, *A&A*, 132, 203
- Henry, G. W., Baliunas, S. L., Donahue, R. A., Soon, W. H., & Saar, S. H. 1997, *ApJ*, 474, 503
- Hsieh, H. H., & Jewitt, D. 2006, *Science*, 312, 561
- Ji, J., Liu, L., Kinoshita, H., Zhou, J., Nakai, H., & Li, G. 2003, *ApJ*, 591, L57
- Ji, J., Liu, L., Kinoshita, H., & Li, G. 2005, *ApJ*, 631, 1191
- Jones, B. W., Sleep, P. N., & Chambers, J. E. 2001, *A&A*, 366, 254
- Kiefer, F., Lecavelier des Etangs, A., Boissier, J., et al. 2014, *Nature*, 514, 462
- Kopparapu, R. K., Ramirez, R., & Kasting, J. F., et al. 2013, *ApJ*, 765, 131; Erratum 770, 82
- Kornet, K., Bodenheimer, P., & Różyczka, M. 2002, *A&A*, 396, 977
- Kovtyukh, V. V., Soubiran, C., Belik, S. I., & Gorlova, N. I. 2003, *A&A*, 411, 559
- Laughlin, G., Chambers, J., & Fischer, D. 2002, *ApJ*, 579, 455

- Lécuyer, C., Gillet, P., & Robert, F. 1998, *Chem. Geol.*, 145, 249
- Loibnegger, B., Dvorak, R., & Cuntz, M. 2017, *AJ*, 153, 203
- Meier, R., & Owen, T. C. 1999, *Space Sci. Rev.*, 90, 33
- Ng, Y. K., & Bertelli, G. 1998, *A&A*, 329, 943
- Noble, M., Musielak, Z. E., & Cuntz, M. 2002, *ApJ*, 572, 1024
- Rappaport, S., Vanderburg, A., Jacobs, T., et al. 2018, *MNRAS*, 474, 1453
- Raymond, S. N., & Izidoro, A. 2017, *Icarus*, 297, 134
- Rickman, H., Fouchard, M., Froeschlé, C., & Valsecchi, G. B. 2008, *Cel. Mech. Dyn. Astron.*, 102, 111
- Saffe, C., Gómez, M., & Chavero, C. 2005, *A&A*, 443, 609
- Simpson, F. 2017, *MNRAS*, 468, 2803
- Thébault, P., Marzari, F., & Scholl, H. 2002, *A&A*, 384, 594
- Turnbull, M. C., & Tarter, J. C. 2003, *ApJS*, 145, 181
- Van Belle, G. T., & von Braun, K. 2009, *ApJ*, 694, 1085
- Vermeij, G. J. 2017, *Current Biol.*, 27, 3178
- Welsh, B. Y., & Montgomery, S. 2013, *PASP*, 125, 759
- Zuckerman, B., & Song, I. 2012, *ApJ*, 758, 77

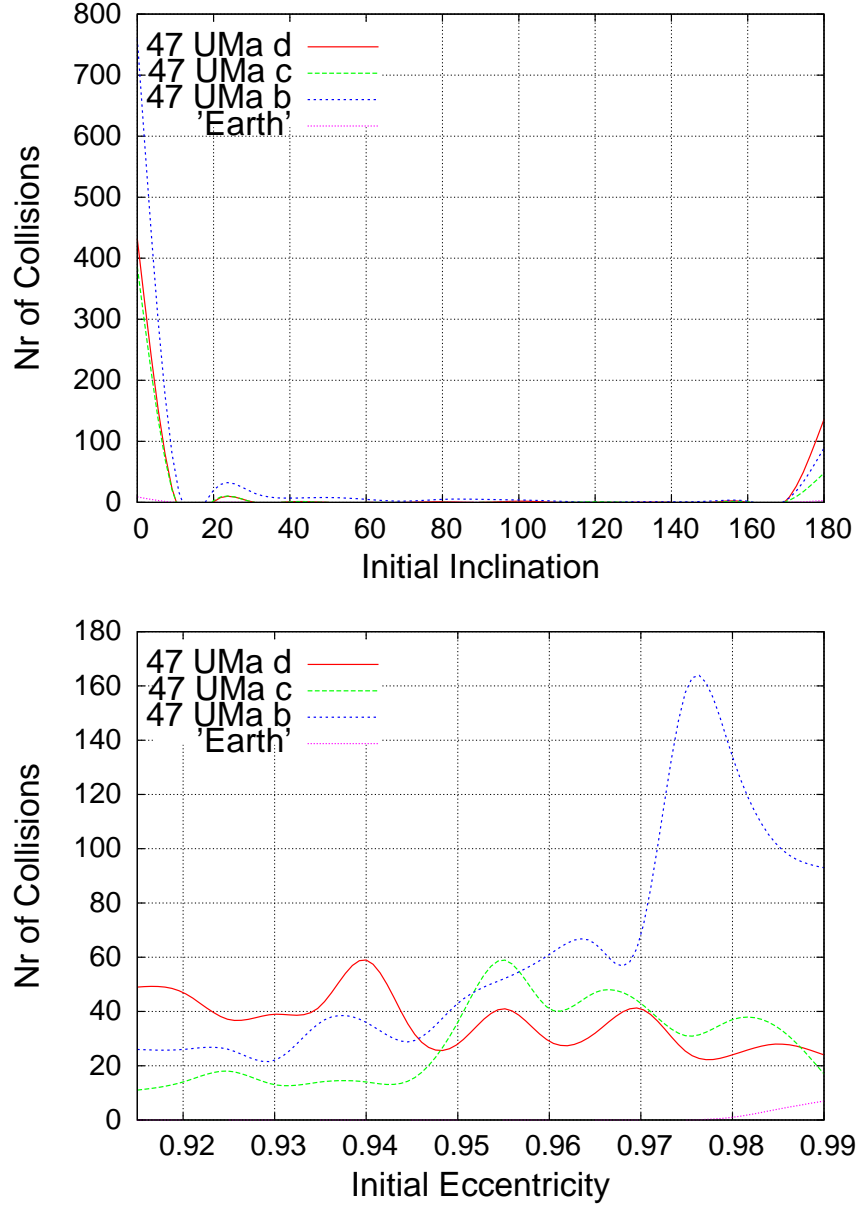


Fig. 1.— Number of collisions with the three 47 UMa giant planets and the fictitious Earth-mass planet at 1 au; furthermore,  $a_{\text{ini,comet}} = 80$  au is assumed. The most massive planet 47 UMa b undergoes most collisions with the comets. Collision with comets of initially small inclinations ( $i < 20^\circ$ ) is most common for all planets (top panel). Moreover, the initial eccentricity of the comets has a significant influence on the collision probability (bottom panel). Comets with initially low eccentricity ( $e < 0.945$ ) cannot reach the inner planetary system. Thus, the number of collisions for comets with these initial conditions is higher for the outermost planet 47 UMa d. As soon as the initial eccentricity exceeds 0.945, comets can reach the inner planetary system and thus experience close encounters with 47 UMa b. The number of collisions peaks at 160 observed collisions with planet b for an initial eccentricity of the comets 0.975. For this value of initial eccentricity, the comets have an initial perihel distance of 2.0 au, which is slightly inside of the orbit of planet b.

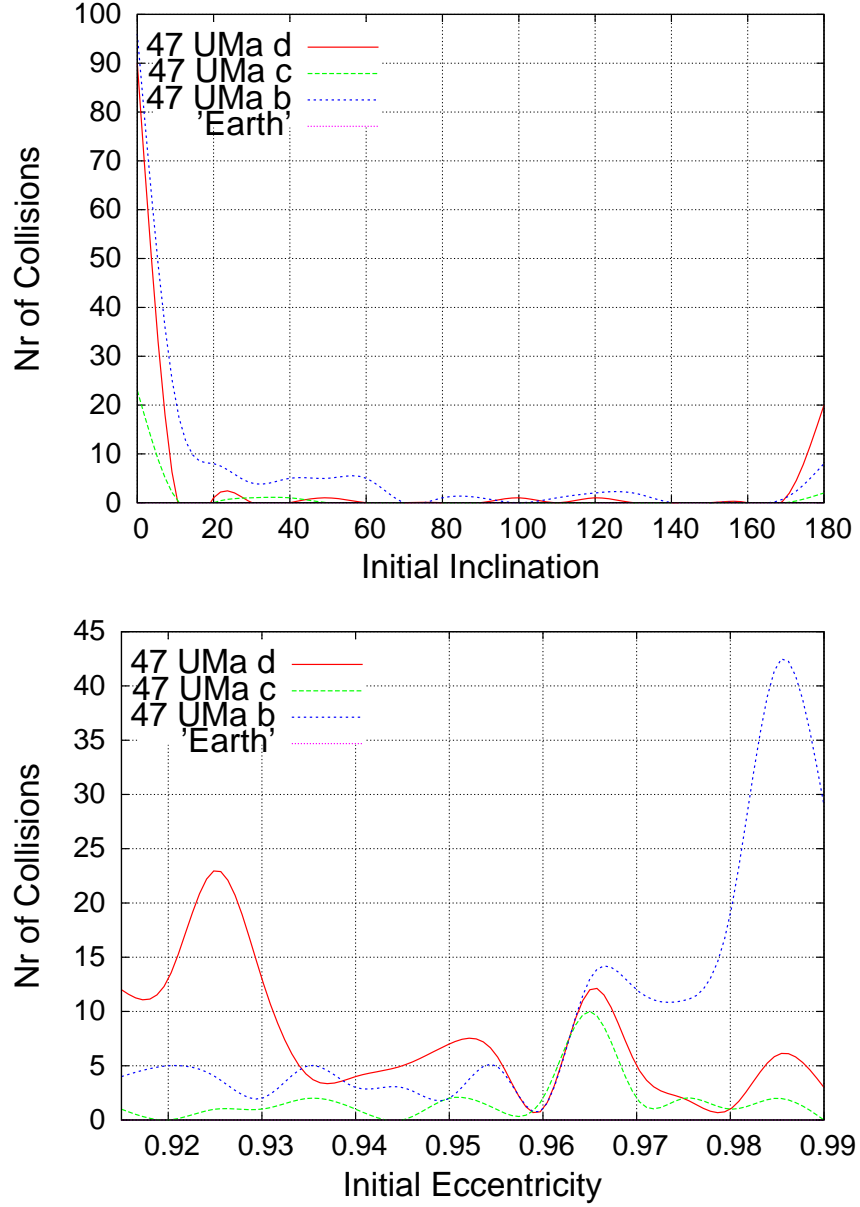


Fig. 2.— Same as Fig. 1, however the comets are started with an initial semi-major axis of  $a_{\text{ini,comet}} = 120$  au. The peak of collisions for comets with initial eccentricities of 0.925 for the outermost planet 47 UMa d shows that now a large number of comets is only able to reach the far-out orbit of this planet, which encounters the majority of collisions.

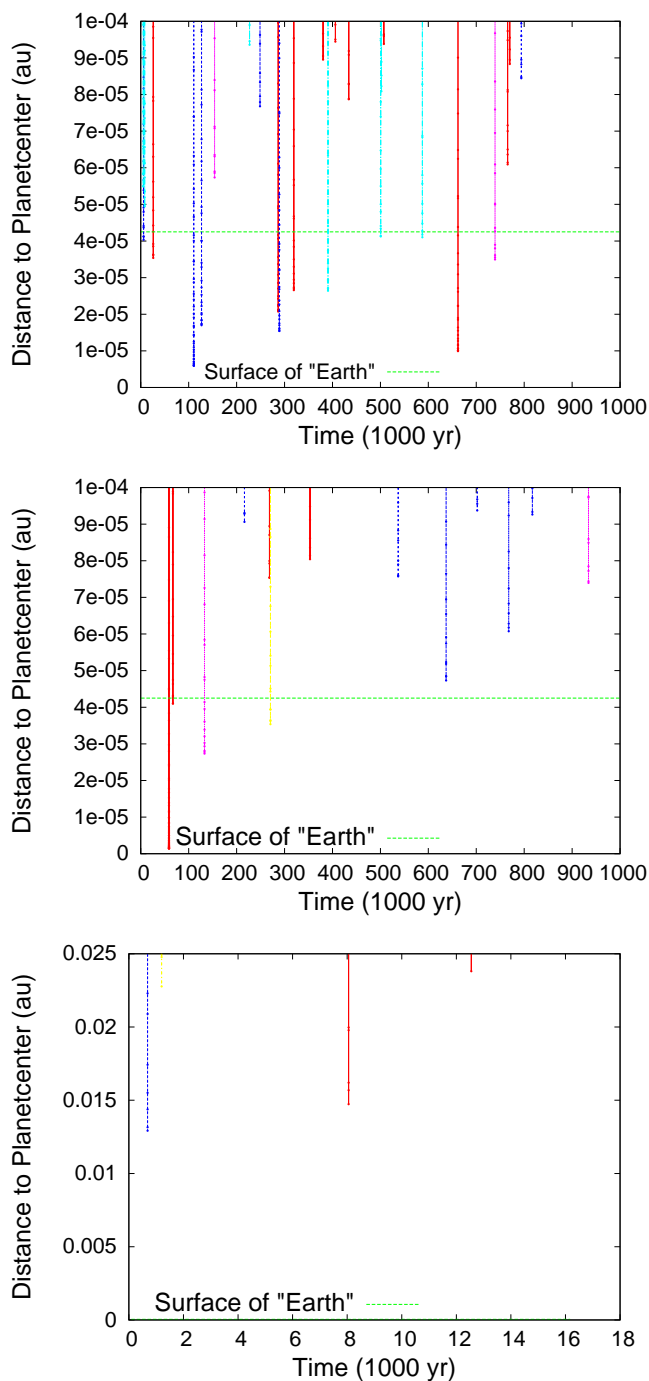


Fig. 3.— The three plots convey the real collisions with the Earth-mass planet at different locations, which are: 1 au (top panel), 1.25 au (middle panel), and 1.584 au, the ‘Hilda’-planet (bottom panel). Collisions with the comets, treated as massless test particles, already occur during the first 1 Myr of integration. The green lines mark the surface of the planet. Note that all lines crossing the green line denote real collisions. It is found that the number of collisions decreases as the Earth-mass planet is put closer to the orbit of the most massive planet, 47 UMa b. Note the different ranges for the  $y$ -axes. Regarding the ‘Hilda’-planet, no real collisions with the planet occur this close to 47 UMa b.

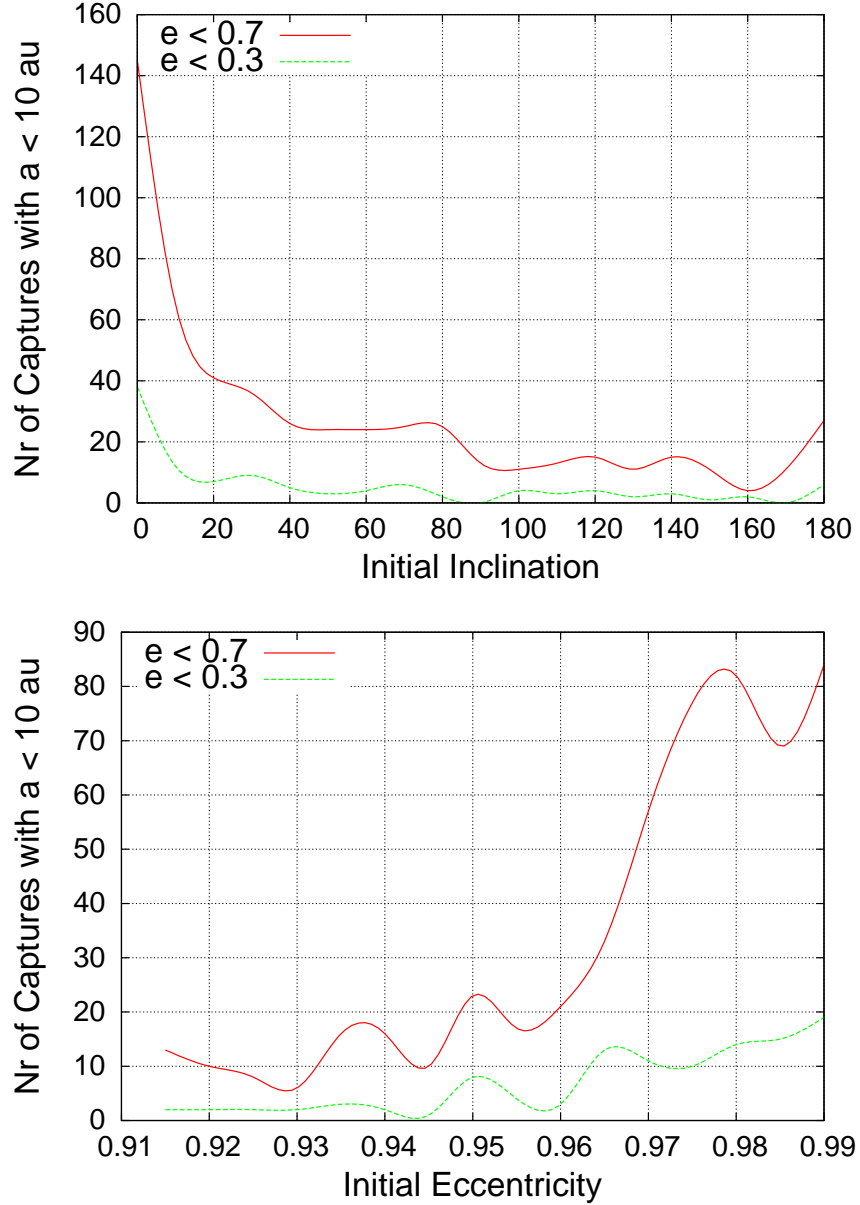


Fig. 4.— Number of captures of comets in orbits with  $a < 10$  au and, respectively,  $e < 0.7$  and  $e < 0.3$  after an integration time of 1 Myr. Results are given for different values of initial inclination (top) and initial eccentricity (bottom). Note that captures occur for comets of all types of initial conditions. Nevertheless, the number of comets scattered to an orbit with the desired values is highest for comets with small initial inclinations and high initial eccentricities. Only comets with high eccentricity are able to reach the inner parts of the system and interact with the most massive planet 47 UMa b, the main perturber capable of scattering the small bodies into orbits with low semi-major axis and eccentricity.

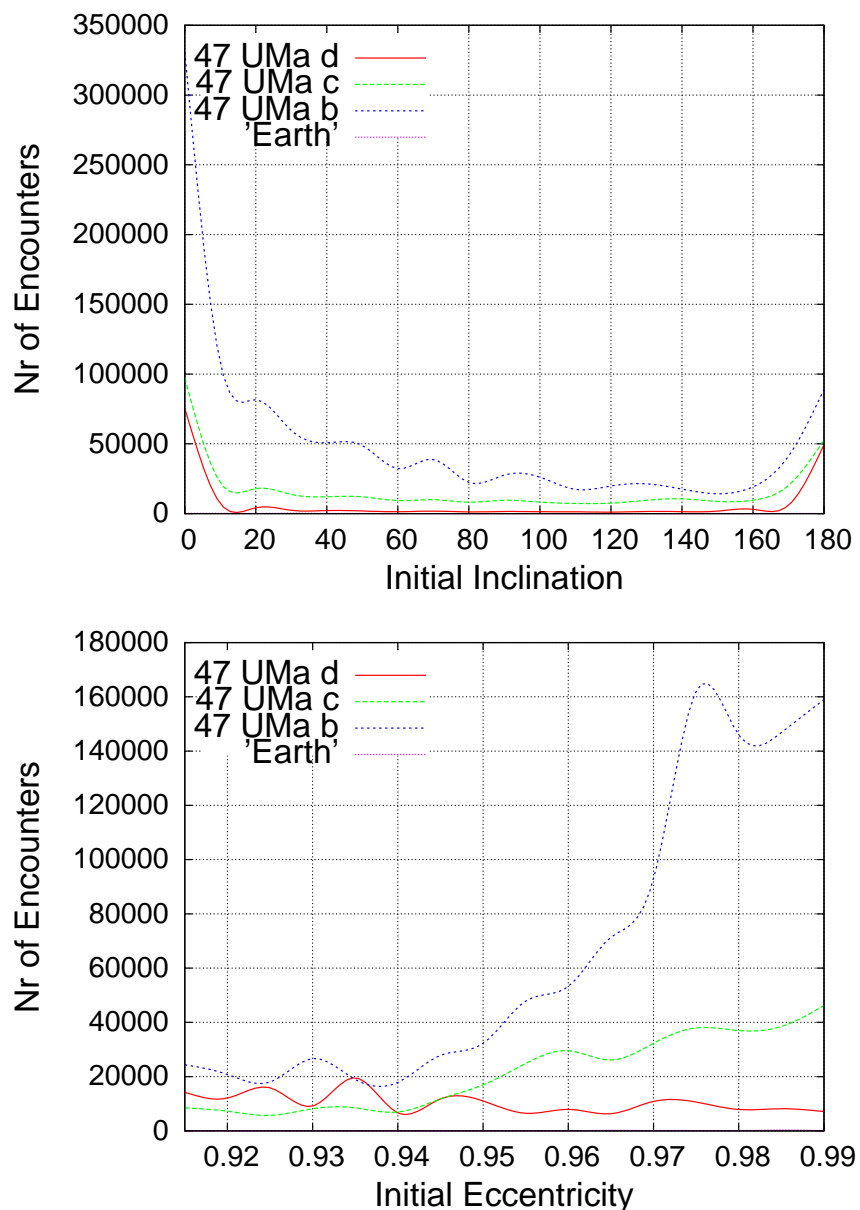


Fig. 5.— Number of encounters of the Earth-mass planet with the various 47 UMa giant planets after it was put in a resonant orbit with 47 UMa b, the most massive planet of the system. Note that the encounters of the Earth-mass planet with the giant planets are very rare. Planet 47 UMa b, the most massive planet, experiences most encounters, and thus has the biggest influence on cometary scattering.

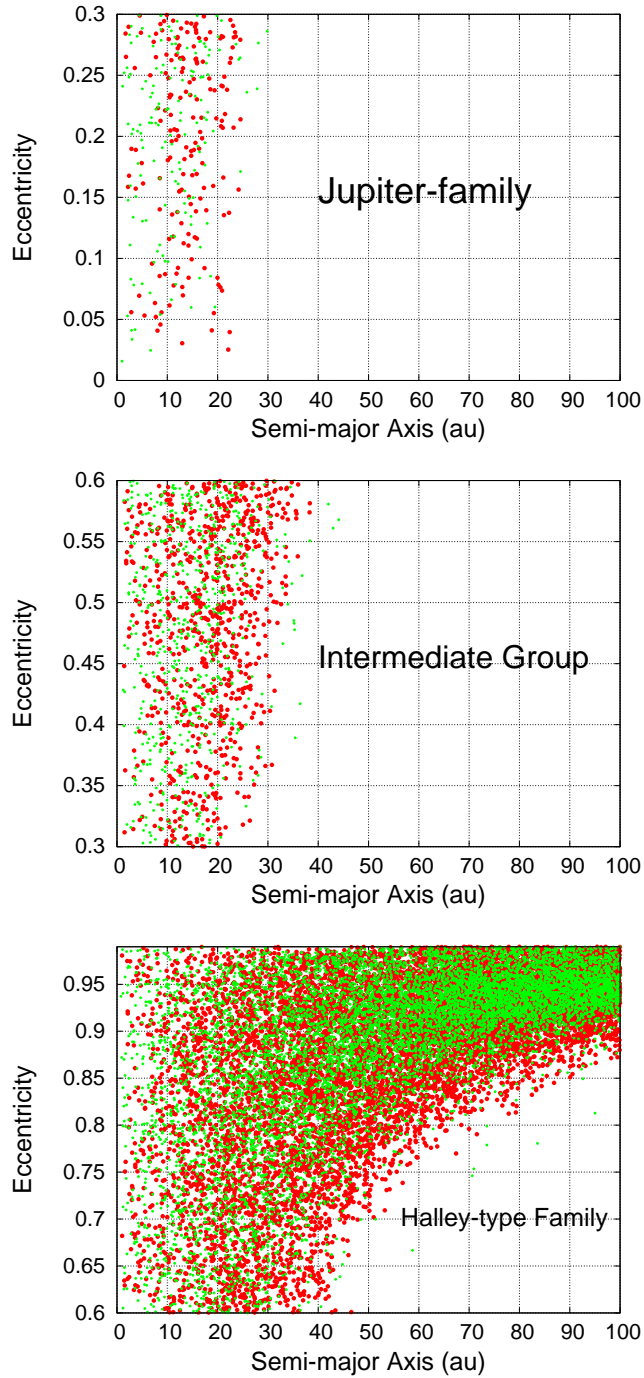


Fig. 6.— Distribution of the orbital elements semi-major axis and eccentricity for the comets after an integration time of 1 Myr. The green and red dots correspond to comets ending up on prograde and retrograde orbits, respectively. The distribution is close to uniform. Both prograde and retrograde comets are found in orbits with relatively small eccentricities and semi-major axes.

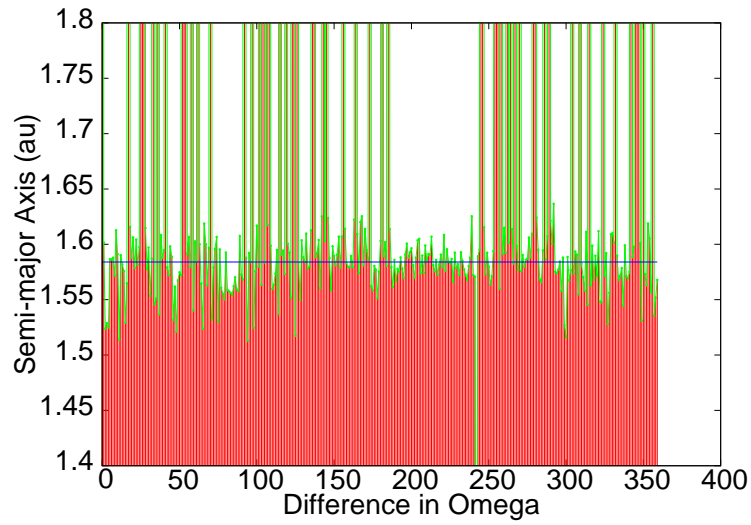


Fig. 7.— Attained semi-major axes ( $y$ -axis) versus the differences in the perihelion of the gas giant and the planet,  $\Delta(\omega_{\text{giant}} - \omega_{\text{planet}})$  ( $x$ -axis); the latter are equally distributed between  $1^\circ$  and  $360^\circ$ . The results refer to 360 fictitious massless ‘Hilda’-planets after an integration time of 1 Myr. Two stable windows are identified.

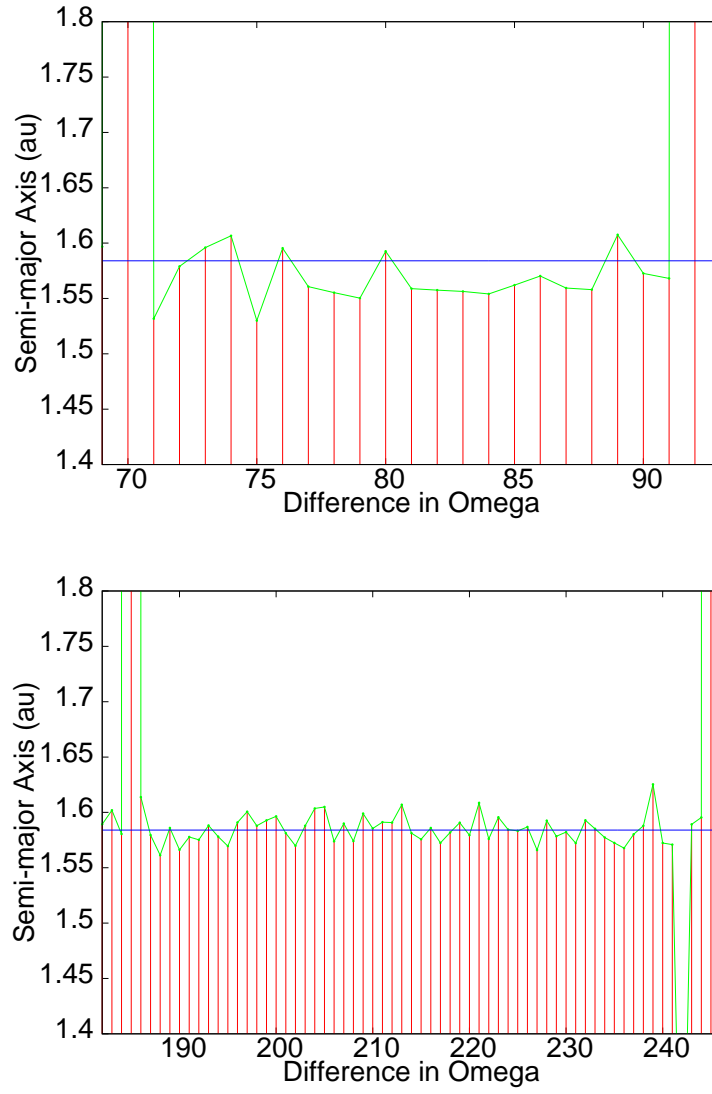


Fig. 8.— Zoomed-in results of Fig. 7 for a small window around  $80^\circ$  (top) and a larger window around  $215^\circ$  (bottom). Axes as in Fig. 7.

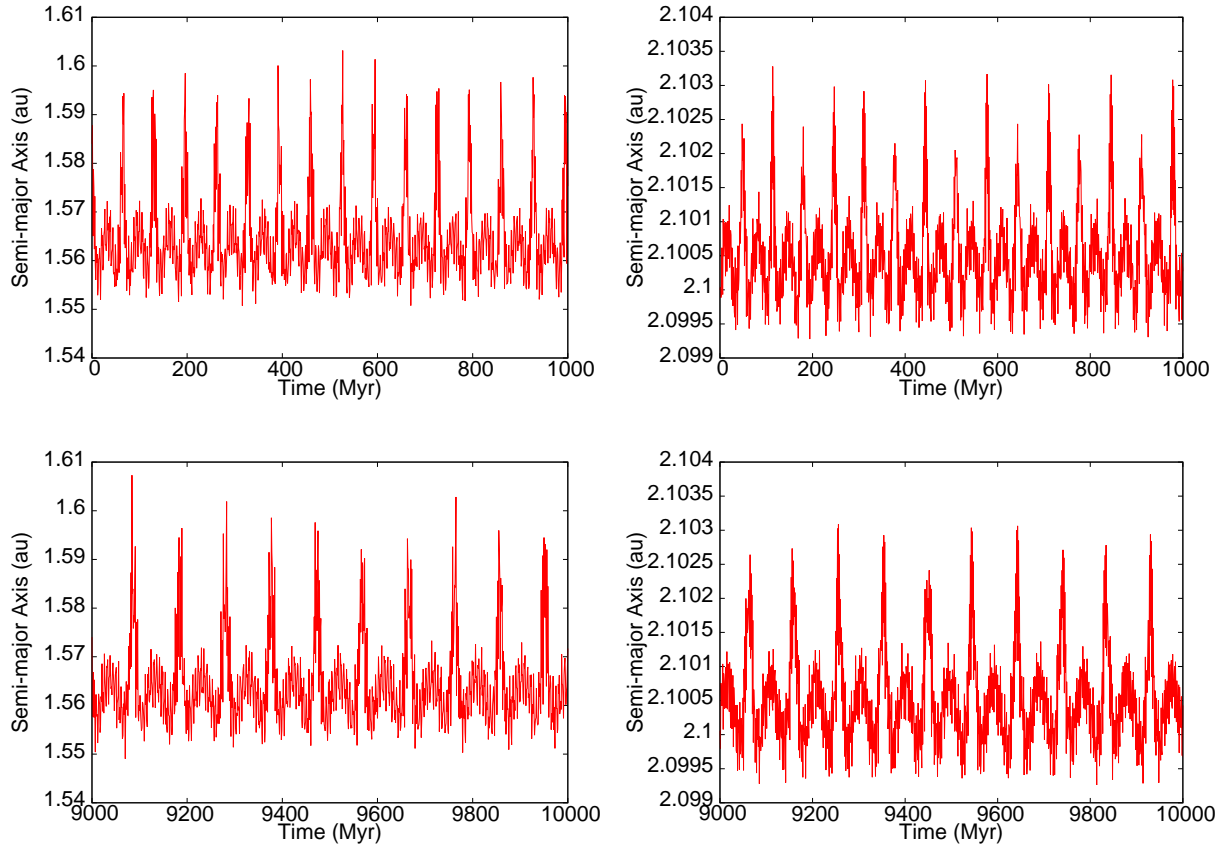


Fig. 9.— Time evolution of the semi-major axis for the ‘Hilda’-planet (upper panel, left) and the gas giant (upper panel, right) for the first hundreds of millions of years. Results for the time interval between 9 to 10 Gyr for the ‘Hilda’-planet (lower panel, left) and the gas giant (lower panel, right) are given as well.

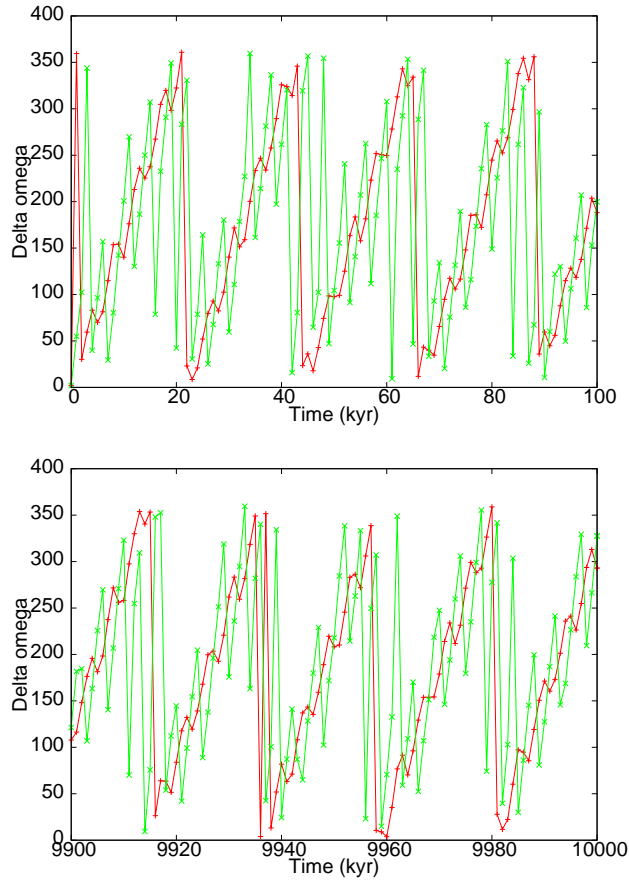


Fig. 10.— Comparison of the time evolution of the difference  $\tilde{\omega}_{\text{planet}} - \tilde{\omega}_{\text{Hilda}}$  for the first 100 kyr and last 100 kyr during the 10 Myr integration.  $\Delta\omega$  is depicted as a function of time. The red line and green line indicate the gas giant and the ‘Hilda’-planet, respectively.

Table 1. Stellar Parameters

Parameter	Unit	Value
Spectral Type	...	G1 V
$T_{\text{eff}}$	(K)	5890
$M_*$	( $M_{\odot}$ )	1.03
$R_*$	( $R_{\odot}$ )	1.17
Metallicity	(% solar)	110
Age	(Gyr)	6.03
$d_{\text{in}}$ (HZ)	(au)	0.91
$d_{\text{out}}$ (HZ)	(au)	2.13

Note. — All variables have their usual meaning. Here  $d_{\text{in}}$  and  $d_{\text{out}}$  indicate the limits of the optimistic HZ, also referred to as RVEM limits; see Kopparapu et al. (2013). However, the outer part of the HZ is unavailable for hosting planets as they would be orbitally unstable due to the gravitational influence of 47 UMa b.

Table 2. 47 UMa Planets

Name	Alternate Name	$a$	$e$	$m$	Discovery
...	...	(au)	...	( $M_J$ )	...
47 UMa b	Taphao Thong	2.1	0.032	2.53	Butler & Marcy (1996)
47 UMa c	Taphao Kaew	3.6	0.098	0.54	Fischer et al. (2002)
47 UMa d	...	11.6	0.16	1.64	Gregory & Fischer (2010)

Table 3. 47 UMa Planet Data

Name	$R_{\text{Hill}}$	$R_{\text{Hill}}$	$r$
...	(au)	( $10^6$ km)	( $10^3$ km)
47 UMa b	0.195	29.23	93.9
47 UMa c	0.200	29.94	56.1
47 UMa d	0.934	139.7	81.2

Note. — Hill radii and planetary radii for the known planets of 47 UMa. Intermediate values are given based on the densities  $\rho_1 = 1 \text{ g cm}^{-3}$  and  $\rho_2 = 2 \text{ g cm}^{-3}$ .

Table 4. Parameter Ranges for the 47 UMa Comet Integrations

Quantity	Lower Bound	Upper Bound	Increment
Semi-major axis $a$ (au)	80	200	10
Eccentricity $e$	0.915	0.990	0.005
Inclination $i$ ( $^\circ$ )	0	180	10

Table 5. Water Transport

...	nr (comets)	nr (coll)	%EOs (1 Myr)	%EOs (6 Gyr)	GLs (6 Gyr)
1 au	2 165 972	12	0.000016	0.093	61.7
1.25 au	3 368 691	9	0.000012	0.073	48.5
‘Hilda’	68 429 091	0	0	0	0

Note. — Overview on the water transport for the different integrations. Numbers are about comets for the full range of inclinations and an initial semi-major axis of 80 au. The amount of water transported is given for a timespan of 1 Myr as well as for the 47 UMa system’s lifetime of 6 Gyr through extrapolation. Results are expressed relative to Earth’s Oceans (%EOs) and the Great Lakes (GLs).

Table 6. Water Transport, cont’d

...	nr (comets)	nr (coll)	%EOs (1 Myr)	%EOs (6 Gyr)	GLs (6 Gyr)
1 au	2 362 287	13	0.000017	0.107	70.5
1.25 au	3 524 063	12	0.000016	0.093	61.7
‘Hilda’	189 883 894	0	0	0	0

Note. — Same as in Table 5, but for all initial semi-major axes in the assumed range (see Table 4 and Sect. 4.5). The results show similar trends as before.